

Title: SPHERICAL COMPRESSION OF A MAGNETIC FIELD

Author(s): C. M. Fowler

RECEIVED

AUG 26 1996

OSTI

DISCLAIMER

This report was prepared as an account of work sponsored by an agency of the United States Government. Neither the United States Government nor any agency thereof, nor any of their employees, makes any warranty, express or implied, or assumes any legal liability or responsibility for the accuracy, completeness, or usefulness of any information, apparatus, product, or process disclosed, or represents that its use would not infringe privately owned rights. Reference herein to any specific commercial product, process, or service by trade name, trademark, manufacturer, or otherwise does not necessarily constitute or imply its endorsement, recommendation, or favoring by the United States Government or any agency thereof. The views and opinions of authors expressed herein do not necessarily state or reflect those of the United States Government or any agency thereof.

Submitted to: Seventh International Conference on Megagauss Magnetic Field Generation and Related Topics August 5-10, 1996 Sarov (Arzamas-16), RUSSIA

MASTER



Los Alamos NATIONAL LABORATORY

Los Alamos National Laboratory, an affirmative action/equal opportunity employer, is operated by the University of California for the U.S. Department of Energy under contract W-7405-ENG-36. By acceptance of this article, the publisher recognizes that the U.S. Government retains a nonexclusive, royalty-free license to publish or reproduce the published form of this contribution, or to allow others to do so, for U.S. Government purposes. The Los Alamos National Laboratory requests that the publisher identify this article as work performed under the auspices of the U.S. Department of Energy.

DISTRIBUTION OF THIS DOCUMENT IS UNLIMITED

VM

**DISCLAIMER**

**Portions of this document may be illegible  
in electronic image products. Images are  
produced from the best available original  
document.**

## SPHERICAL COMPRESSION OF A MAGNETIC FIELD

C.M.Fowler

Los Alamos National Laboratory, Los Alamos, NM, USA

### Introduction

In an interesting paper, Rutkevich [1] obtained the electromagnetic wave solution for the compression of a magnetic field contained by an imploding, perfectly conducting cylindrical shell or liner. The magnetic and electric susceptibilities were taken as constant. The solution was obtained by Laplace transforms. In his paper, he also considered the corresponding plane problem when driving together two perfectly conducting, parallel plates that confine a magnetic field. He compared the method of solution obtained by Laplace transforms with that obtained by the method of characteristics which was used to obtain the original solution [2]. He concluded his paper by noting that the transform method is more versatile than the characteristic method. Somewhat later, Bodulinskii and Medvedev [3] obtained a solution for the wave structure generated when an initial magnetic field is compressed by the implosion of a conducting spherical liner. Again, the solution was obtained by transform methods.

In this paper we outline the solution to the spherical problem using the method of characteristics. The utility of this method is described for some other situations.

### Imploding Liner

Figure 1. gives the details of the idealized problem solved by Bodulinskii and Medvedev. A perfectly conducting sphere, initial radius  $a$ , implodes with radial velocity  $v$ . An initial azimuthal field is set up by a total current  $I$  passing through the thin, non-resistive diametral filament from A to B, and returns over the surface of the sphere with current density  $j$ . The authors found a solution in spherical coordinates when the field has only an azimuthal component,  $B_\phi \equiv B$ , and the electric field only a  $\theta$  component,  $E_\theta \equiv E$ . Both components are assumed to be independent of the azimuthal angle  $\phi$ . Maxwell's equations show that the combinations  $B \sin \theta$  and  $E \sin \theta$  depend only on  $R$  and  $t$ , and lead to the following relations:

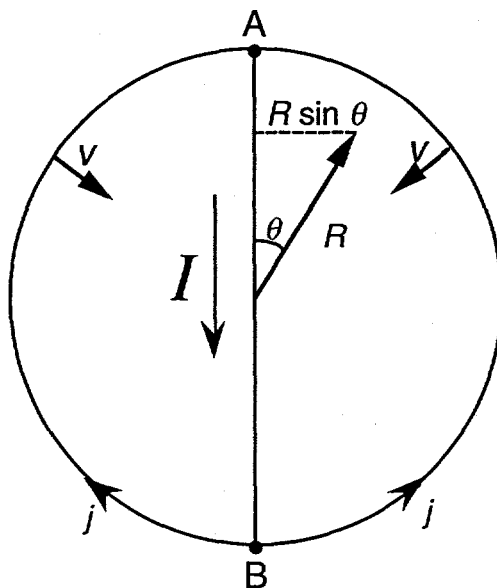


Fig. 1. Cross-section of a sphere imploding with velocity  $v$ . Current  $I$  flows from A to B through a diametral filament and returns on the spherical surface with areal density  $j$ .

$$\frac{\partial \beta}{\partial R} + \frac{1}{c^2} \frac{\partial \varepsilon}{\partial t} = 0 ; \quad \frac{\partial \varepsilon}{\partial R} + \frac{\partial \beta}{\partial t} = 0 \quad (1)$$

where  $c$  is the velocity of light and

$$\beta = BR \sin \theta ; \quad \varepsilon = ER \sin \theta. \quad (2)$$

As noted the dependent variables in (1) are functions only of  $R$  and  $t$ . Eqs (1) can be rearranged as follows:

$$\begin{aligned} \left( \frac{\partial}{\partial R} + \frac{1}{c} \frac{\partial}{\partial t} \right) (\varepsilon + c\beta) &= 0 \\ \left( \frac{\partial}{\partial R} - \frac{1}{c} \frac{\partial}{\partial t} \right) (\varepsilon - c\beta) &= 0 \end{aligned} \quad (3)$$

These are the characteristic equations for the field variables,  $\varepsilon \pm c\beta$ , cast in the form of directional derivatives ( $\pm c$ ). Thus the quantity  $\varepsilon + c\beta$  is constant along "characteristic lines" of slope  $+c$ , and  $\varepsilon - c\beta$  along lines of slope  $-c$ .

Figure 2. shows characteristic lines of slopes  $\pm 1/c$ , along which the quantities  $\varepsilon \pm c\beta$  are constant. The boundary and initial conditions for the idealized problem described above are:

$$\begin{aligned} \varepsilon &= 0 \text{ at } R = 0 ; \quad \varepsilon = v\beta \text{ at the moving boundary} \\ \varepsilon &= 0, \quad I = I_0 \text{ and } \beta = \frac{\mu I_0}{2\pi} \text{ at } t = 0 \end{aligned} \quad (4)$$

The solution proceeds in a straightforward but tedious fashion, as follows:

We divide the space time region into zones as shown in Figure 2., with the aim of finding the values of  $\varepsilon$  and  $\beta$  on the boundaries. This is sufficient information to find the values of  $\varepsilon$  and  $\beta$  at arbitrary interior points, as follows:

For points in the interior zones, such as  $z$ , on the plus characteristic,  $\varepsilon_z + c\beta_z = \varepsilon_i + c\beta_i$ , while on the minus characteristic,  $\varepsilon_z - c\beta_z = \varepsilon_{i-1} - c\beta_{i-1}$ . Here the zone subscripts are used to denote values at the spherical boundary. With these equations and the relation  $\varepsilon = v\beta$  at the boundary, we find for point  $z$ :

$$\begin{aligned} \varepsilon_z &= \frac{1}{2} c [(1-r)\beta_i - (1+r)\beta_{i-1}] \\ \beta_z &= \frac{1}{2} [(1-r)\beta_i + (1+r)\beta_{i-1}] \end{aligned} \quad (5)$$

with

$$r \equiv -v/c. \quad (v \text{ is negative here.})$$

For points in the right zones, such as  $W$ , both  $\varepsilon$  and  $\beta$  have the same values as those on the boundary zone,  $i$ . This follows immediately with use of the two characteristics,  $WR$  and  $WR'$ .

For points in the left zone, such as  $Y$ , a similar analysis gives values of  $\varepsilon$  and  $\beta$  equal to that at  $R = 0$ . Since  $\varepsilon$  is zero at this boundary, there are no electric fields in these zones.

The next step relates boundary values on zone  $i$  to those on zone  $i-2$ . First, from Eq(4),  $\varepsilon_i = v\beta_i$ ;  $\varepsilon_{i-2} = v\beta_{i-2}$ . Following the negative characteristic from  $Q$  to  $P$ , and with  $\varepsilon_P = 0$  (Eq(4)), we obtain  $-c\beta_P = \varepsilon_{i-2} - c\beta_{i-2}$ . Then from the plus characteristic from  $P$ , we have  $+c\beta_P = \varepsilon_i + c\beta_i$ . If we substitute  $r = -v/c$  ( $v$  is negative), then these equations give:

$$\beta_i = \frac{1+r}{1-r} \beta_{i-2} \equiv \gamma \beta_{i-2}. \quad (6)$$

Once the values of  $\beta$  for the first two zones are known,  $\beta_i$  for the remaining zones can be obtained from Eq(6). For a point A in zone  $i = 0$ , from the characteristic OA we have  $c\beta_0 = c\mu_0 l/2\pi = \varepsilon_A + c\beta_A = (c+v)\beta_A = c(1-r)\beta_A$ . A similar analysis, using the two characteristics OC and CB gives the same value for  $\beta_B$ . Thus

$$\beta_1 = \beta_2 = \frac{\mu_0 l_0}{2\pi(1-r)} \quad (7)$$

The solution of Eq(6) with the initial values of Eq(7) gives:

$$\begin{aligned} \beta_i &= \frac{\mu_0 l_0}{2\pi(1-r)} (\sqrt{\gamma})^i ; i \text{ even} \\ \beta_i &= \frac{\mu_0 l_0}{2\pi(1-r)} (\sqrt{\gamma})^{i-1} ; i \text{ odd} \end{aligned} \quad (8)$$

From Eq(8), if  $i$  is even, then  $i-1$  is odd and the values of  $\beta$  that go into Eq(5) for the central zone are

$$\beta_i = \frac{\mu_0 l_0}{2\pi(1-r)} (\sqrt{\gamma})^i ; \beta_{i-1} = \frac{\mu_0 l_0}{2\pi(1-r)} (\sqrt{\gamma})^{i-2}$$

Similarly, when  $i$  is odd,

$$\beta_i = \frac{\mu_0 l_0}{2\pi(1-r)} (\sqrt{\gamma})^{i-1} ; \beta_{i-1} = \frac{\mu_0 l_0}{2\pi(1-r)} (\sqrt{\gamma})^{i-1}$$

With these values substituted in Eq(5), we obtain the following values for the central space-time zones:

$$\begin{aligned} \varepsilon_z &= 0 ; \beta_z = \frac{\mu_0 l_0}{2\pi} (\sqrt{\gamma})^i ; i \text{ even} \\ \varepsilon_z &= \frac{\mu_0 l_0}{2\pi(1-r)} v (\sqrt{\gamma})^{i-1} ; \beta_z = \frac{\mu_0 l_0}{2\pi(1-r)} (\sqrt{\gamma})^{i-1} ; i \text{ odd} \end{aligned} \quad (9)$$

Values of  $\beta$  for the inner zone, as at point Y, are the same as those at  $R = 0$  ( $\varepsilon$  for these points is zero). To obtain these values we have on the characteristic lines from P that  $c\beta_P = \varepsilon_i + c\beta_i$  or  $\beta_P = \beta_i(1-r)$ , and from Eq(8), for the inner zones:

$$\begin{aligned} \beta_P = \beta_Y &= \frac{\mu_0 l_0}{2\pi} (\sqrt{\gamma})^i ; \varepsilon_Y = 0 ; i \text{ even} \\ \beta_P = \beta_Y &= \frac{\mu_0 l_0}{2\pi} (\sqrt{\gamma})^{i-1} ; \varepsilon_Y = 0 ; i \text{ odd} \end{aligned} \quad (10)$$

Equations (8), with  $\varepsilon = v\beta$ , (9) and (10) give values for  $\varepsilon$  and  $\beta$  for the outer, central, and inner zones, respectively. Figure 3 shows pairs of  $\beta$  and  $\varepsilon/c$  values obtained from these equations where we have set  $\mu_0 l_0/2\pi = 1$  and  $r = 0.1$  ( $v = -0.1c$ ).  $\beta$  is the upper number;  $\varepsilon/c$  the lower.

The space-time zones are a natural consequence of the method of characteristics, although it is also natural to use the same zoning system when the wave equation is solved by other means, such as by various transforms. The characteristic method is particularly useful if there is a change of velocity of the boundary, such as shown at point A of Figure 3. The velocity change is felt above the characteristic AB. Although field values along characteristic EF are computed from the original boundary condition, values along ED are influenced by the

different boundary condition along AC. The field values above AB are still determined algebraically, but close attention must be paid to the more complicated structure in ABJ where the influence of both boundary conditions is still felt.

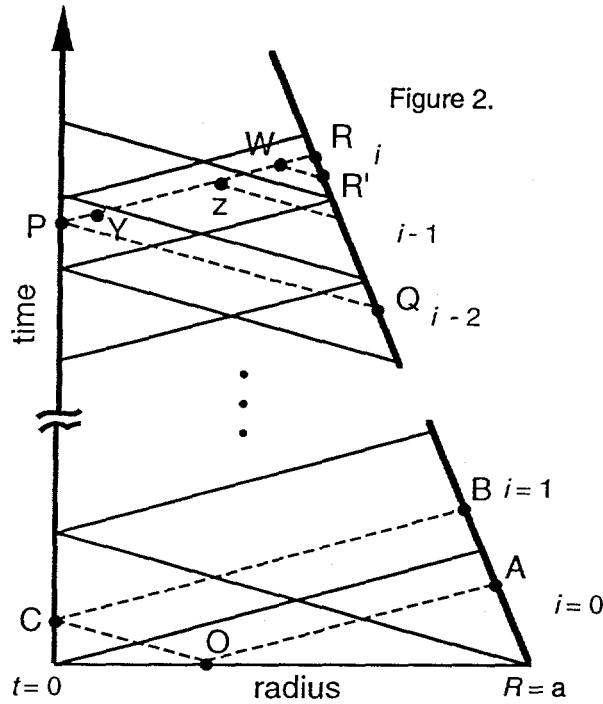


Figure 2.

Fig. 2. Characteristic lines, slopes  $1/c$ , for the interior of a sphere whose surface moves inward with a velocity  $v$  from an initial radius  $a$ .

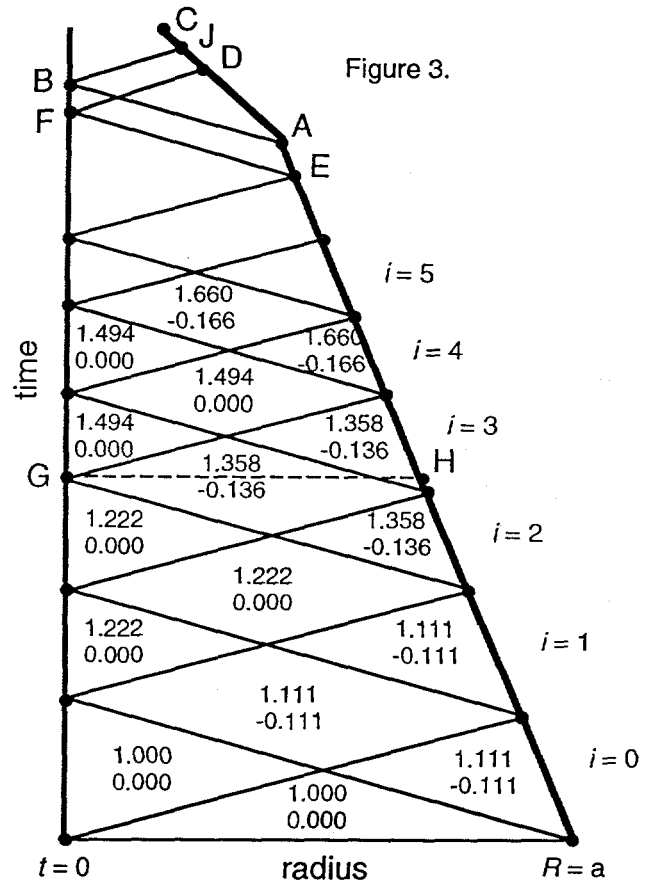


Figure 3.

Fig. 3. Normalized values of  $\beta$  (upper values) and  $\epsilon$  for the space-time zones. Note the change in liner velocity at A.

Analytic expressions usually require knowing the time at the various zone boundaries. No matter what method of solution is used, finding these values is usually a very tedious matter – even for the simple case shown on Figure 3 before the velocity change at A. For example, consider the flux contained by the sphere. For the diametral plane of Figure 1, the flux  $\phi$  when the radius has reached an arbitrary radius  $R_1$ , is

$$\phi = \int_{\theta_1}^{\theta_2} \int_0^{R_1} BR dR = \int_{\theta_1}^{\theta_2} d\theta \int_0^{R_1} \frac{\beta dR}{\sin \theta} = \int_{\theta_1}^{\theta_2} \frac{d\theta}{\sin \theta} \int_0^{R_1} \beta dR$$

The  $\theta$  integral diverges for  $\theta_1$  and  $\theta_2$  equal to  $\pm 90^\circ$ , the ideal case treated here and the flux is therefore infinite from this factor. However, the radial integral can be shown to be independent of time. Since this is also true of the  $\theta$  contribution, there is a kind of "flux conservation." Although specialized, the easiest radial integral evaluations occur along lines such as GH where  $\beta$  is constant. The problem thus reduces to finding the radius at H for the particular time G. Graphically, the problem is simple. Initially  $\beta = 1.00$  and  $R = 1.00$  and the radial flux integral  $\phi_0 = 1.00$  in these units. We estimate that  $H = 0.73$ . Thus the radial flux integral is  $\phi \cong (1.358)(0.73) = 0.99^+$ , in essential agreement with  $\phi_0$ . However, it is a rather messy job to obtain  $R_1$  in terms of time analytically. The problem is much messier for arbitrary times, where more than one zone is involved with different values of  $\beta$  in the zones. However, numerically

the solution still proceeds in a straightforward manner, even with velocity changes such as shown at A on Fig 3.

### The non-linear plane problem

In Reference 2 it was shown that, in vacuum, the combinations  $E \pm cB$  were invariant along lines of slope  $+c$ . Here, the only space variable was the Cartesian variable  $x$ . The corresponding non-linear case was considered in Reference 4. Since the distribution of that report is somewhat limited, we reproduce here some of the results.

When the field variable  $D$  is a function only of  $E$ , and  $B$  is a function only of  $H$ , the following relations are obtained

$$\left(\frac{\partial}{\partial x} + s \frac{\partial}{\partial t}\right) \left[ \int \left(\frac{\partial D}{\partial E}\right)^{1/2} dE \pm \int \left(\frac{\partial B}{\partial H}\right)^{1/2} dH \right] = 0; \quad s = \left(\frac{\partial D}{\partial E} \cdot \frac{\partial B}{\partial H}\right)^{1/2} \quad (11)$$

Thus, the bracketed terms are invariant along the characteristic curves with local derivatives in the direction of  $\pm s$ . With appropriate given boundary values, the equations may be solved numerically by standard iterative techniques. It may be noted that, in vacuum, the characteristic directions are constant (straight lines) with slopes  $\pm c$ , and that the invariants reduce to  $E \pm cB$ , as they should.

The power of the characteristic method is illustrated by another example in Reference 4. The constitutive relations linking  $B$  and  $D$  to  $E$  and  $H$  were chosen to make all the characteristic curves with negative slope be straight lines of the same slope  $c$ . This condition led to the result that the characteristics with positive slope were also straight lines, but with varying slopes. In the interest of obtaining an analytic solution to the problem a special (and highly unrealistic) form was adapted for the constitutive relations. Interesting wave propagation results were obtained, reminiscent of some hydrodynamic situations, such as the existence of a centered simple wave and a shock-like envelope.

### Summary

Transform methods are exceedingly versatile in solving problems of the type considered here, provided the problems remain linear. The characteristic method is basically restricted to problems with a single space variable (at least at present) and then mainly in plane situations. However, the method has advantages, particularly in numerical computations, in handling changes in boundary velocity and particularly in situations where the constitutive relations are non-linear.

### References

1. I.M. Rutkevich "The Electromagnetic Field in a Cavity Undergoing Compression", PMM Vol.31, No.3, 1967, p.552-559.
2. C.M. Fowler, W.B. Gam and R.S. Caird "Production of Very High Magnetic Fields by Implosion", *J. Appl. Phys.*, Vol.31, No.3, 1960, p.588-594.
3. V.K. Bodulinskii and Yu.A. Medvedev "Compression of Magnetic Field in an Imploding Spherical Cavity", *Zhurnal Prikladnoi Mekhaniki i Tekhnicheskoi Fiziki*, No.6, 1970, p.114-115.
4. C.M. Fowler "Losses in Magnetic Flux Compression Generators, Part 2: Radiation Losses", LANL Report LA-9956-MS, Part 2, 1988.